arXiv:1405.1007v3 [cond-mat.other] 17 Jun 2014

Andreev-Majorana bound states in superfluids.

Mikhail Silaev[1, 2] and G.E. Volovik[1, 3]

[1] *Low Temperature Laboratory, Aalto University, P.O. Box 15100, FI-00076 Aalto, Finland*
[2] *Institute for Physics of Microstructures RAS, 603950 Nizhny Novgorod, Russia*
[3] *Landau Institute for Theoretical Physics, acad. Semyonov av., 1a, 142432, Chernogolovka, Russia*

(Dated: June 18, 2014)

We consider Andreev-Majorana (AM) bound states with zero energy on surfaces, interfaces and vortices in different phases of the p-wave superfluids. We discuss the chiral superfluid ^{3}He-A, and time reversal invariant phases: superfluid ^{3}He-B, planar and polar phases. The AM zero modes are determined by topology in bulk, and they disappear at the quantum phase transition from the topological to non-topological state of the superfluid. The topology demonstrates the interplay of dimensions. In particular, the zero-dimensional Weyl points in chiral superfluids (the Berry phase monopoles in momentum space) give rise to the one-dimensional Fermi arc of AM bound states on the surface and to the one-dimensional flat band of AM modes in the vortex core. The one-dimensional nodal line in the polar phase produces the two-dimensional flat band of AM modes on the surface. The interplay of dimensions also connects the AM states in superfluids with different dimensions. For example, the topological properties of the spectrum of bound states in the three-dimensional ^{3}He-B is connected to the properties of the spectrum in the two-dimensional planar phase (thin film).

PACS numbers:

Contents

I. Introduction 1

II. Andreev-Majorana edge states in 2+1 gapped topological superfluids 2
A. Chiral ^{3}He-A film 3
B. Time-reversal invariant planar phase 3

III. AMBS on surface of 3+1 gapped topological superfluid 4
A. ^{3}He-B edge states from bulk topology 5
B. ^{3}He-B edge states from topology of planar phase 5
C. Evolution of edge state at non-topological QPT 6
D. Evolution of edge state at topological QPT 6

IV. AMBS on surface of 3+1 Weyl superfluid. Fermi arc 7
A. Andreev-Majorana Fermi arc on the boundary of Weyl superfluid 7
B. Andreev-Majorana Fermi arcs on soliton and domain wall 8

V. Topological superfluids with lines of zeroes. AM surface flat band. 8
A. Flat band of AM modes on surface of polar phase 8
B. Flat band on surface of model graphite 10

VI. AM modes on vortices in chiral $2+1$ superfluids 10

VII. AM flat band in a vortex in Weyl superfluids 11

VIII. AMBS in ^{3} He-B vortex 12
A. From planar phase to B-phase 12
B. AMBS on B-phase vortices with broken symmetry 12

IX. Conclusion 14

X. Acknowledgements 14

References 14

I. INTRODUCTION

Majorana fermions are ubiquitous for superconductors and fermionic superfluids. The Bogoliubov- de Gennes equation for fermionic Bogoliubov-Nambu quasiparticles can be brought to a real form by unitary transformation. This implies the linear relation between the particle and antiparticle field operators, which is the hallmark of a Majorana fermion. The fermionic statistics and Cooper pair correlations give rise to Majorana fermions, irrespective of geometry, dimensionality, symmetry and topology[1–3]. The role of topology is to protect gapless Majorana fermions, which play the major role at low temperature, when the gapped degrees of freedom are frozen out. For some combinations of geometry, dimensionality and symmetry these Majorana fermions behave as emergent massless relativistic particles. This suggests that Majorana fermions may serve as building blocks for construction of the Weyl particles of Standard Model[4].

Here we consider the gapless Majorana fermions, which appear as Andreev bound states on the surfaces of superfluids and on topological objects in superfluids: quantized vortices, solitons and domain walls. In all cases the bound states are formed due to the subsequent Andreev

reflections of particles and holes. The key factor for the formation of ABS on the small defect with the size of the order of coherence length is a non-trivial phase difference of the order parameter at the opposite ends of particle trajectory. In general it depends on the structure of the order parameter in real and momentum space which can be rater complicated. The possibilities for the formation of ABS are rather diverse, several of them are shown in in Fig.1. The particularly interesting are the case when ABS are topologically stable, which means that they have stable zero-energy Majorana modes which cannot be eliminated by the small perturbation of the system parameters.

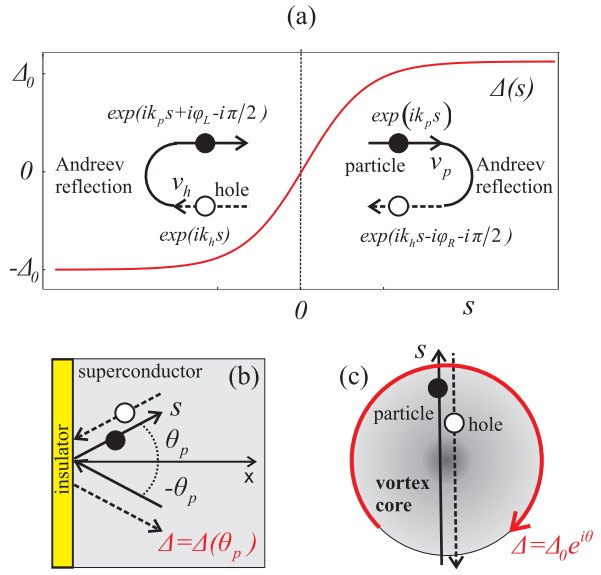

FIG. 1: Schematically shown formation of Andreev bound states localized (a) on domain wall, (b) on the edge, (c) inside the vortex core. In all cases the mechanism is the subsequent particle-hole conversions via Andreev reflections at the opposite ends of the trajectory s. The reflected particle (hole) picks up the phase of the order parameter $\varphi_R(-\varphi_L)$ and flips the group velocity direction $\boldsymbol{v}_p(\boldsymbol{v}_h)$ as shown in the panel (a). In general the wave vectors of particle and hole in the bulk are slightly different $k_{p,h} = k_F \pm E/v_F$ where k_F and v_F are Fermi momentum and velocity, E is the energy. In case if the order parameter phase difference is $\phi_R - \phi_L = \pi$ the closed loop can be formed even for $k_e = k_h$, that is for the zero energy $E = 0$. In cases (b,c) the phase difference appears due to the momentum dependence of the gap function and the phase winding around the vortex core correspondingly.

General properties of fermionic spectrum in condensed matter and particle physics are determined by topology of the ground state (vacuum). The classification schemes based on topology[5–11] suggest the classes of topological insulators, fully gapped topological superfluids/superconductors and gapless topological media. In Refs.[9–11] the classification is based on topological properties of matrix Green's function, while the other schemes explore the properties of single particle Hamiltonian and thus are applicable only to systems of free (non-interacting) fermions. Among the fully gapped topological superfluids there is the time-reversal invariant superfluid ^{3}He-B, thin films of chiral superfluid ^{3}He-A and thin films of the time-reversal invariant planar phase of superfluid ^{3}He. The main signature of topologically nontrivial vacua with the energy gap in bulk is the existence of zero-energy edge states on the boundary, at the interface between topologically distinct domains[12,13] and in the vortex cores[14]. For superfluids and superconductors these are Andreev-Majorana bound states (AMBS). These are mainly propagating fermionic quasiparticles, which have relativistic spectrum at low energy[15–20]. However, for special geometries and dimensions, the Andreev-Majorana bound state represents the isolated non-propagating midgap state, called the Majorana zero mode (or Majorino[21]). It is not a fermion, since it obeys a non-Abelian exchange statistics[22]. This in particular occurs for the AMBS in the vortex core of chiral p-wave superfluid-superconductor in 2+1 dimensions[23].

The gapless AMBS takes place also on the surfaces, interfaces and in the vortex cores of the gapless topological media. Among them there are chiral superfluid ^{3}He-A with Weyl points, the time-reversal invariant planar phase with Dirac points and the time-reversal invariant polar phase with line of zeroes. The spectrum of Andreev-Majorana bound states there is non-relativistic and exotic: the zeroes of AMBS spectrum form Fermi arcs[24–27] and flat bands[28–35].

II. ANDREEV-MAJORANA EDGE STATES IN 2+1 GAPPED TOPOLOGICAL SUPERFLUIDS

The p-wave superfluid ^{3}He has been discovered in 1972. However till now there is little understanding of superfluid ^{3}He films. The information on recent experiments in confined geometry can be found in review[36]. In thin films the competition is expected between the chiral superfluid ^{3}He-A and time-reversal invariant planar phase, both acquiring the gap in the spectrum in quasi-two-dimensional case due to transverse quantization.

The fermionic spectra in both the 2D A phase and the planar phase have non-trivial topological properties. These topological states provide the examples of systems featuring generic topological phenomena. In particular the analog of integer quantum Hall effect exist in the 2D A phase where the internal orbital momentum of Cooper pairs plays the role of time reversal symmetry breaking magnetic field. In the time reversal invariant planar phase the quantum spin Hall effect can be realized. In close analogy with the 2d electronic systems the topological invariant is determined by the number of fermionic edge modes with zero energy. In the superfluid systems the edge zero modes are the ABS localized at the superfluid/vacuum boundary or at the interfaces and domain walls separating superfluid states with different topological properties. Below we discuss in detail the topological properties and ABS for the 2D A phase and the planar

phase.

A. Chiral ^{3}He-A film

The order parameter in spatially homogeneous time reversal symmetry breaking ^{3}He-A phase is given $\hat{\Delta} = \sigma_x(p_x \pm ip_y)$ where σ_x is spin Pauli matrix and the $p_{x,y}$ are momentum projections to the anisotropy plane. Such order parameter describes the triplet Cooper pairs with zero spin $S_z = 0$ and non-zero oribital momentum $L_z = \pm 1$ projections onto the anisotropy axis. The non-zero L_z plays the role of internal magnetic field breaking the time-reversal symmetry of the systems. Confined in zy plane the 2D state of A phase is a fully gapped system. By the analogy with 2D electronic gase in quantized magnetic field the gapped ground states (vacua) in 2+1 or quasi 2+1 thin films of ^{3}He-A are characterized by the following topological invariant[37–41]:

$$N = \frac{e_{ijk}}{24\pi^2}\ \mathbf{tr}\left[\int d^3p\ G\partial_{p_i}G^{-1}G\partial_{p_j}G^{-1}G\partial_{p_k}G^{-1}\right]. \quad (1)$$

Here $G = G(p_x, p_y, \omega = ip_0)$ is the Green's function matrix, which depends on Matsubara frequency p_0; the integration is over the whole (2+1)-dimensional momentum-frequency space $p_i = (p_x, p_y, p_0)$, or over the Brillouin zone and p_0 in crystals. The expression (1) is the extension of the TKNN invariant invented by Thouless *et al.* to describe the topological quantization of Hall conductance[42,43].

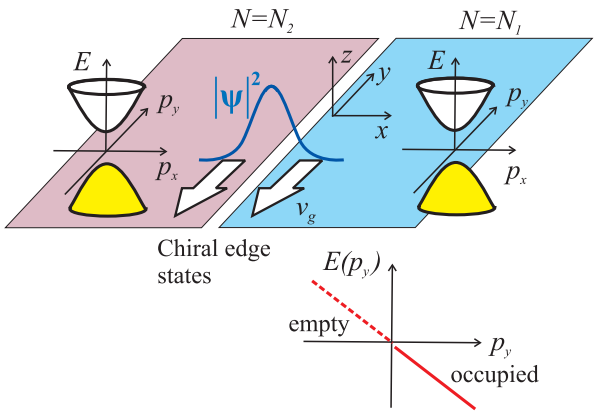

FIG. 2: Schematic picture of the interface between two films of chiral $p_x + ip_y$ superfluid with values N_1 and N_2 of topological invariant (1). The interface contains chiral AMBS with spectrum $E = E(p_y)$, which move with group velocity $v_g = dE(p_y)/dp_y$. In general the algebraic sum of branches (the number of left moving − the number of right moving fermions) is $N_2 - N_1$. On the lower panel the chiral branch of spinless AMBS is shown given by Eq.(3), when $N_2 = 1$ and $N_1 = 0$. For the spinful case in Eq.(2) there are two anomalous branches of spectrum of edge states $E(p_y)$ which are degenerate over spin. The chiral branches produce an equilibrium mass current flowing along the interface.

The advantage of the topological approach is that one can choose for consideration the simplest form of Green's function, which has the same topological properties and can be obtained from the complicated one by continuous deformation. For a single layer of ^{3}He-A film one can choose

$$G^{-1} = ip_0 + \tau_3\left(\frac{p^2}{2m} - \mu\right) + c\sigma_z\left(\tau_1 p_x + \tau_2 p_y\right). \quad (2)$$

where $p^2 = p_x^2 + p_y^2$. The Pauli matrices $\tau_{1,2,3}$ and $\sigma_{x,y,z}$ correspond to the Bogoliubov-Nambu spin and ordinary spin of ^{3}He atom respectively; the parameter c characterizes the amplitude of the superconducting order parameter. The weak coupling BCS limit corresponds to $mc^2 \ll \mu$. In this limit one has $c = \Delta/p_F$, where Δ is the gap in the spectrum and p_F is Fermi momentum, $p_F^2/2m = \mu$.

It is also instructive to consider the simplified case when there is only a single spin component, which corresponds to the fully spin polarized $p_x + ip_y$ superfluid:

$$G^{-1} = ip_0 + \tau_3\left(\frac{p^2}{2m} - \mu\right) + c\left(\tau_1 p_x + \tau_2 p_y\right). \quad (3)$$

We call this case as spinless fermions. The topological invariant (1) for the state in Eq.(3) with $\mu > 0$ is $N = 1$, while for the state with $\mu < 0$ one has $N = 0$. According to the bulk-surface correspondence, at the interface between these two phases there must be the branch of the Andreev-Majorana edge states, which crosses zero energy level[15,44], see Fig. 2.

In the spinful case of Eq.(2), both spin components equally contribute to the topological invariant, and one has $N = 2$ for $\mu > 0$ and $N = 0$ for $\mu < 0$. Therefore there must be two branches of the Andreev-Majorana edge states, which cross zero energy level. In general case the algebraic sum of anomalous branches (the number of left moving minus the number of right moving fermions) satisfies the index theorem, $n_L - n_R = N(x > 0) - N(x < 0)$.

B. Time-reversal invariant planar phase

Alternative to the 2D chiral A phase in thin films of superfluid ^{3}He the time-reversal invariant planar phase[45] can become stable. While this phase has not been identified experimentally yet, in recent experiments[36,46–49] strong suppression of the transverse gap has been observed.

The order parameter which describes the spatially homogeneous time reversal invariant planar phase has the form $\hat{\Delta} = p_y + i\sigma_z p_x$. In this phase, the order parameters is anisotropic and vanishes for the $\mathbf{p} \parallel \mathbf{z}$ direction, transverse to the film. Nevertheless, confined in 2D when $p_z = 0$ this system is gapful.

Being time-reversal invariant the planar phase has zero topological invariant of the type given by Eq.(1). How-

ever it has an extra discrete symmetry, namely a combination of a π spin rotation around z-axis followed by a $\pi/2$ phase rotation. This modifies the topological classification, adding extra $\mathbb{Z}$ topological invariant obtained by Volovik and Yakovenko in Ref. 41. This invariant gives rise to the intrinsic spin-Hall effect illustrated in Fig. 3.

An extra motivation to study this particular case of the planar phase is that it can be considered as a corner stone for a dimensional reduction scheme which can be applied to general class-DIII topological superconductors. In the next section we discuss that the topological properties of a 3D system and an embedded (2+1)D system, which exist in any time-reversal invariant cross section of the momentum space, are connected. As an application of such a reduction we derive a generalized index theorem for 3D topological superconductors, which provides an example of the bulk-boundary correspondence in odd spatial dimensions.

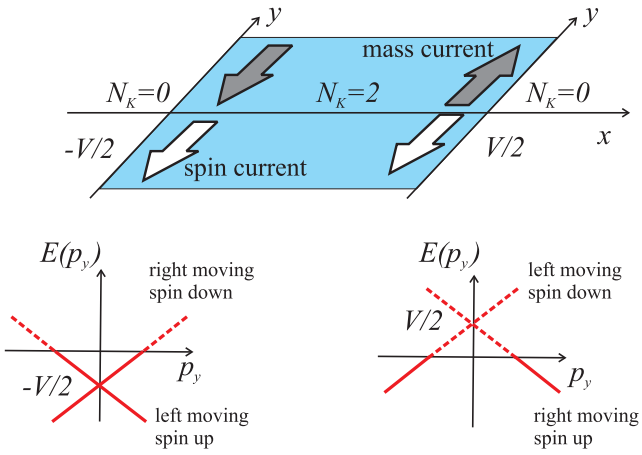

FIG. 3: An illustration of the intrinsic spin-current quantum Hall effect due to Andreev-Majorana edge states in the stripe of the planar phase film with topological invariant $N_K = 2$ in Eq. (6). As distinct from ^{3}He-A in Fig. 2, the anomalous branches with different spin projections have opposite slopes. This gives rise to the quantized spin Hall effect without magnetic field, instead of the quantized Hall effect in ^{3}He-A film[41,50].

In the single layer case, the simplest expression for the planar phase Green's function $G(p_0, p_x, p_y)$ is determined by

$$G^{-1} = ip_0 + \tau_3 \left(\frac{p^2}{2m} - \mu \right) + c\tau_1(\sigma_x p_x + \sigma_y p_y) \,. \quad (4)$$

This phase is symmetric under time reversal. The two spin components have opposite chiralities, as can be seen from identity

$$\sigma_x p_x + \sigma_y p_y = \frac{1}{2}(\sigma_x + i\sigma_y)(p_x - ip_y) + \frac{1}{2}(\sigma_x - i\sigma_y)(p_x + ip_y) \,. \quad (5)$$

That is why the contributions of the two spin components to the topological invariant (1) cancel each other, $N = 0$. But the planar phase is still topologically non-trivial because of the discrete Z_2-symmetry between the two spin components in Eq.(5). Due to this symmetry the matrix $K = \tau_3\sigma_z$ commutes with the Green's function, which allows us to introduce the symmetry protected topological invariant[41,50]:

$$N_K = \frac{e_{ijk}}{24\pi^2} \, \mathbf{tr} \left[K \int d^3p \; G\partial_{p_i} G^{-1} G\partial_{p_j} G^{-1} G\partial_{p_k} G^{-1} \right] . \quad (6)$$

This invariant is robust to deformations, if the deformations are K-symmetric. For the state (4) with $\mu > 0$ one has $N_K = 2$. For the general case of the quasi 2D film with multiple layers of the planar phase, the invariant N_K belongs to the group Z. The magnetic solid state analog of the planar phase is the 2D time reversal invariant topological insulator, which experiences the quantum spin Hall effect without external magnetic field[12].

Fig. 3 demonstrates Andreev-Majorana edge states on two boundaries of the stripe of the single layer of planar phase film. As distinct from ^{3}He-A in Fig. 2, the anomalous branches with different spin projections are not degenerate: they have opposite slopes, which corresponds to the zero value of the invariant $N = 0$ in Eq.(1). In case of superconductor with planar phase symmetry, the invariant N_K determines quantization of spin Hall effect. In applied voltage V the spectra on two boundaries shift in opposite directions, changing the population of branches. This produces the imbalance in the spin currents carried by edge states on two boundaries, giving rise to the non-zero total spin-current J^z_x (current of z-projection of spin along x-axis). This is in the origin of quantized spin Hall effect in the absence of magnetic field[41,50,51]:

$$J^z_x = \sigma^{\rm spin}_{xy} E_y \quad , \quad \sigma^{\rm spin}_{xy} = \frac{N_K}{4\pi} \,. \quad (7)$$

In this time reversal invariant system the electric current QHE is absent. The topological charge N in Eq.(1), which determines quantization of the Hall conductance in the absence of magnetic field[40], is $N = 0$, and the currents of different spin populations cancel each other.

The mass and spin currents carried by AM edge state in p-wave superfluids have been considered in Refs.[52,53].

III. AMBS ON SURFACE OF 3+1 GAPPED TOPOLOGICAL SUPERFLUID

Fully gapped $3 + 1$ fermionic systems - topological insulators and topological superconductors - are now under extensive investigation. The interest to such systems is revived after identification of topological insulators in several compounds[12].

These systems are characterized by the gapless fermionic states on the boundary of the bulk insulator or at the interface between different states of the

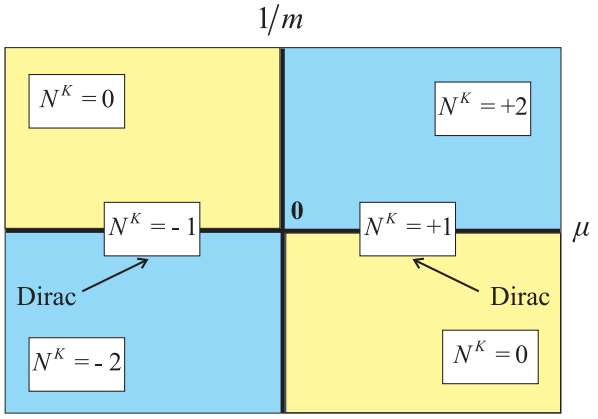

FIG. 4: Phase diagram of topological states of triplet superfluid of ^{3}He-B type in equation (9) in the plane $(\mu, 1/m)$. States on the line $1/m = 0$ correspond to the Dirac vacua, which Hamiltonian is non-compact. Topological charge of the Dirac fermions is intermediate between charges of compact ^{3}He-B states. The line $\mu = 0$ marks topological quantum phase transition, which occurs between the weak coupling ^{3}He-B (with $\mu > 0$, $m > 0$ and topological charge $N_K = 2$) and the strong coupling ^{3}He-B (with $\mu < 0$, $m > 0$ and $N_K = 0$). This transition is topologically equivalent to quantum phase transition between Dirac vacua with opposite mass parameter $M = \pm|\mu|$. The gap in the spectrum becomes zero at this transition. The line $1/m = 0$ separates the states with different asymptotic behavior of the Hamiltonian at infinity: $H(\mathbf{p}) \to \pm\tau_3 p^2/2m$. The transition across this line occurs without closing the gap.

insulator. Historically, the topological insulators with fermionic zero modes at the interface have been introduced in works[54]. An example of the fully gapped topological superfluids is the B phase of superfluid ^{3}He. Much attention has been devoted to the investigation of bound fermion states on surface of ^{3}He-B. The presence of Andreev-Majorana surface states in ^{3}He-B can be probed through anomalous transverse sound attenuation[55–58], and surface specific heat measurements[59,60]. These AM bound states are supported by the non-zero value of the topological invariant in ^{3}He-B[20] and have two - dimensional relativistic massless Dirac spectrum[16–19,24].

A. ^{3}He-B edge states from bulk topology

The topological superfluid/superconductor of the ^{3}He-B type are described by topological invariant N_K, which is protected by symmetry:

$$N_K = \frac{e_{ijk}}{24\pi^2}\,\mathbf{tr}\left[K\int d^3p\; H^{-1}\partial_{p_i}HH^{-1}\partial_{p_j}HH^{-1}\partial_{p_k}H\right]. \tag{8}$$

Here $H(\mathbf{p})$ is the Hamiltonian, or in case of interacting system the inverse Green's function at zero frequency $H(\mathbf{p}) = G^{-1}(\omega = 0, \mathbf{p})$, and K is matrix which commutes or anti-commutes with $H(\mathbf{p})$.

The proper model Hamiltonian which has the same topological properties as superfluids/superconductors of the ^{3}He-B class is the following :

$$H = \left(\frac{p^2}{2m} - \mu\right)\tau_3 - c\tau_1\boldsymbol{\sigma}\cdot\mathbf{p}\,, \tag{9}$$

where τ_i and σ_i are again the Pauli matrices of Bogolyubov-Nambu spin and nuclear spin correspondingly. The symmetry K, which enters the topological invariant N_K in (8), is represented by the τ_2 matrix, which anti-commutes with the Hamiltonian: it is the combination of time reversal and particle-hole symmetries of ^{3}He-B. In the limit $1/m = 0$, Eq.(9) transforms to the Dirac Hamiltonian, where the parameter c serves as the speed of light, while ^{3}He-B lives in the opposite limit $mc^2 \ll \mu$. The topological phase diagram in the plane of parameters $\mu, 1/m$ is in Fig. 4.

The mechanism of Andreev-Majorana bound states formation at the edge of ^{3}He-B is clear from the Hamiltonian (9). Let us consider the boundary plane at $x = 0$ as shown schematically in the Fig.(5). Then upon the normal reflection of particles and holes from the boundary some components of the gap function in (9) change sign. Therefore one obtains a non-zero phase of the gap along the effective trajectory as shown in Fig.(1). In particular for the trajectories normal to the boundary $p_{x,y} = 0$ the overall gap function changes the sign leading to the formation of the zero-energy state localized at the boundary.

However this is not the whole story. Indeed if one formally assumes that the Hamiltonian may have either negative effective mass, $m < 0$, or negative chemical potential, $\mu < 0$, the exact solution of the spectral problem yields no zero-energy states as will be discussed below. The hint to the topological origin of the AMBS in ^{3}He-B can be obtained from the topological phase diagram in Fig. 4, which demonstrates that the system undergoes a topological quantum phase transitions as one changes the sign of chemical potential μ or effective mass m.

The domain wall, which separates the states with different values of N_K, should contain the zero energy states – the Andreev-Majorana zero modes.

B. ^{3}He-B edge states from topology of planar phase

To prove the existence of the Andreev-Majorana bound states on the surface of ^{3}He-B or at the interface one can use a dimensional reduction. Let us assume that the boundary plane is at $x = 0$, so that the conserved longitudinal momentum projections are $k_{z,y}$. To find the complete spectrum of bound states $E_b = E_b(k_y, k_z)$ it is enough to consider a set of 2D spectral problems for the cross sections of momentum space

$$k_y\cos\theta + k_z\sin\theta = 0\,, \tag{10}$$

where $2\pi > \theta \geq 0$.

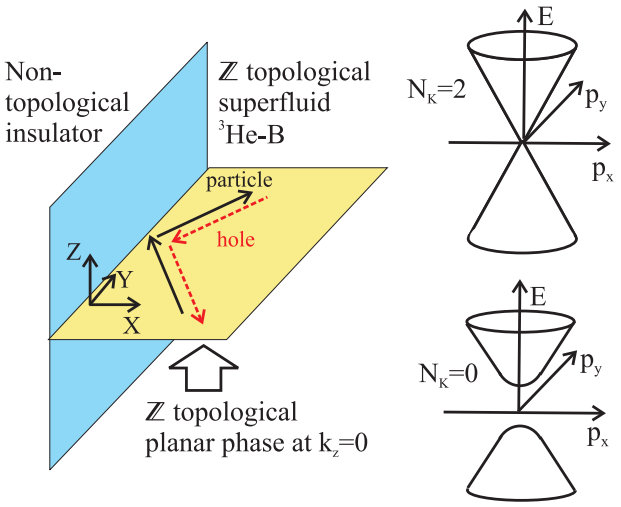

FIG. 5: (Color online) Dimensional reduction of the surface-states spectral problem in 3D to that in the time-reversal invariant cross section of momentum space $k_z = 0$. Reduction from the $\mathbb{Z}$ topological superfluid ^{3}He-B results in the $\mathbb{Z}$ topological planar phase at $k_z = 0$.

An example of such a dimensional reduction to the plane $k_z = 0$ is shown in Fig.5. The $2 + 1$ Hamiltonian in this cross section reduced from the $3 + 1$ phase exactly coincides with the Hamiltonian of the planar phase. Therefore it is classified by the integer-valued topological invariant N_K in Eq.(6), which can be shown to coincide with the topological invariant N_K of the parent 3D ^{3}He-B phase in Eq.(8). The topologically protected Andreev-Majorana states in ^{3}He-B are thus related to the topologically protected edge states in the $2 + 1$ planar phase, see details in Ref.[61].

C. Evolution of edge state at non-topological QPT

Let us consider the spectrum of Andreev-Majorana fermions using the simplest model of the interface between the superfluid and the vacuum, in which the Hamiltonian (9) changes abruptly at the boundary, with the boundary condition $\psi(z = 0) = 0$.

At low energies $|E| \ll \Delta$ their spectrum is helical spectrum, being described by the Hamiltonian $H_{\rm AM} = c(\sigma_y p_x - \sigma_x p_y)$[16]. Interestingly an exact solution of the spectral problem demonstrates[62] that the linear spectrum of AMBS exist up to the merging point with the continuous spectrum of delocalized states.

For $m > 0$ the exact spectrum of Andreev-Majorana fermions $E = \pm p_\perp$ is shown by the red solid line in Fig. 6 for $E > 0$. The bound states are confined to the region $|p_\perp| < \sqrt{2m\mu}$. They disappear when their spectrum merges with the continuous spectrum in bulk. The edge of continuous spectrum is shown by blue dashed line in Fig. 6. If $mc^2 > \mu$ the minimum of the bulk energy spectrum increases monotonically with momentum $p_\perp$,

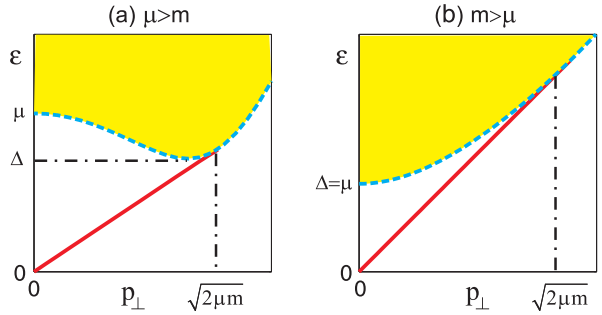

FIG. 6: Spectrum of Andreev-Majorana fermions, localized states on the surface of topological superfluid/superconductor of the ^{3}He-B class (red solid lines) for (a) $\mu > m > 0$ and (b) $m > \mu$. The spectrum of bound states terminates when it merges with continuous spectrum in bulk (yellow color), whose border is shown by blue dashed line. The AM bound states exist for $p_\perp^2 < 2m\mu$.

therefore the bulk gap is

$$\Delta = \mu \quad , \quad mc^2 > \mu \, . \tag{11}$$

If $\mu > mc^2$ the minimum of the bulk energy is non-monotonic function of $p_\perp$ having the minimum at $p_\perp^{min} = \sqrt{2m(\mu - mc^2)}$ where the bulk gap is

$$\Delta = \sqrt{mc^2(2\mu - mc^2)} \quad , \quad 0 < mc^2 < \mu \, . \tag{12}$$

The line $mc^2 = \mu$ marks the non-topological quantum phase transition – the momentum space analog of the Higgs transition[10], when the Mexican hat potential as function of $p_\perp$ emerges for $\mu > mc^2$.

D. Evolution of edge state at topological QPT

Let us first consider the behavior of the spectrum of Majorana fermions at the topological transition at which m crosses zero. When m approaches zero, $m \to 0$, the region of momenta where bound states exist shrinks and finally for $m < 0$, i.e. in the topologically trivial superfluid, no bound states exist any more. Simultaneously the gap in bulk, which at small m is $\Delta \approx \sqrt{2mc^2\mu}$ according to Eq. (12), decreases with decreasing m and nullifies at $m = 0$. This corresponds to the conventional scenario of the topological quantum phase transition, when at the phase boundary between the two gapped states with different topological numbers the gap is closed. The same happens at the TQPT occurring when μ crosses zero (see phase diagram in Fig. 4).

Now let us consider what happens with bound states in the case if the TQPT occurs in the opposite limit, when m changes sign via infinity, i.e. when $1/m$ crosses zero. This topological transition occurs without closing of the gap. In this case the bound states formally exist for all p_x even in the limit $1/m \to 0$. However, in this limit the ultraviolet divergence takes place: the characteristic

length scale of the wave function of the bound state $L \propto \hbar/mc \to 0$. So, if the TQPT from topologically non-trivial to the trivial insulator (or superconductor) occurs without closing the gap, the gapless spectrum of surface states disappears by escaping via ultraviolet. This limit corresponds to formation of zero of the Green's function, $G = 1/(i\omega - H) \to 0$. Such scenario is impossible in the models with the bounded Hamiltonian[63,64], which takes place in approximation of finite number of crystal bands.

On the other hand Green's function zeroes can occur due to the particle interactions. As was found in Ref.[68], classifications of interacting and non-interacting fermionic systems do not necessarily coincide. This is related to zeroes of the Green's function, which according to Ref.[10] contribute to topology alongside with the poles. Due to zeroes the integer topological charge of the interacting system can be changed without closing the energy gap, and it is suggested that this may lead to the occurrence of topological insulators with no fermion zero modes on the interface[63,64].

That is why we expect that the same scenario with escape to the ultraviolet takes place for the interacting systems: if due to zeroes in the Green's function the TQPT in bulk occurs without closing the gap, the spectrum of edge states will nevertheless change at the TQPT, and this change occurs via the ultraviolet.

Finally let us mention, that the magnetic field violates time reversal symmetry, which generically leads to the finite gap (mass) in the spectrum of AM fermions on the surface. At particular orientation of the magnetic field there is still the Z_2 dsicrete symmetry, which supports gapless AMBS[65,66]. This symmetry is spontaneously broken at some critical value of magnetic feild, above which the AM fermions become massive. The surface of ^{3}He-B with massive AM bound states represents the $2+1$ topological "insulator": it is described by the topological invariant in Eq.(1). The line on the surface, which separates the surface domains with different values of this topological invariant, contains $1+1$ gapless AM fermions[67].

IV. AMBS ON SURFACE OF 3+1 WEYL SUPERFLUID. FERMI ARC

Now we move to the AM bound states which appear as edge and vortex states in the gapless topological systems. Here the zeroes in bulk lead to the extended zeroes on the surfaces, interfaces and vortex cores. We start with point zeroes – Weyl points – in chiral superfluids, which produce the lines of zeroes (Fermi arc) on the surface, and the flat band in the vortex core.

A. Andreev-Majorana Fermi arc on the boundary of Weyl superfluid

The topological origin of AM bound states in $3+1$ chiral superfluids can be viewed by extension of the topology of the $2+1$ chiral system in Sec. II to the $3+1$ case. Let us consider for simplicity the spinless fermions, or which is the same, the fermions with a given spin polarization. Then the Green's function in Eq.(2) extended to $3+1$ case is:

$$G^{-1}(\mathbf{p}, p_0) = ip_0 + \tau_3 \left(\frac{p^2}{2m} - \mu \right) + c\left(\tau_1 p_x + \tau_2 p_y\right). \quad (13)$$

where $\mathbf{p} = (p_x, p_y, p_z)$. Let us consider p_z as parameter of the $2+1$ system. Then for each p_z, except for $p_z = \pm p_F$, this Green's function describes the fully gapped $2+1$ system – the "insulator", which is characterized by topological invariant in Eq.(1):

$$N(p_z) = \frac{1}{4\pi^2}\ \mathbf{tr}\left[\int dp_x dp_y dp_0\ G\partial_{p_x}G^{-1}G\partial_{p_y}G^{-1}G\partial_{p_0}G^{-1}\right]. \quad (14)$$

This insulator is topological for $|p_z| < p_F$, where $N(|p_z| < p_F) = 1$, and is topologically trivial for $|p_z| > p_F$, where $N(|p_z| > p_F) = 0$.

At $p_z = \pm p_F$, the invariant (14) is not determined, since the corresponding $2+1$ system is gapless. The bulk $3+1$ superfluid ^{3}He-A has two points in the spectrum $\mathbf{p}_\pm = (0, 0, \pm p_F)$, where energy is zero, see Fig. (7). These nodes in the spectrum are topologically protected, since they represent the monopoles in the Berry phase in momentum space and are characterized by the topological invariant in Eq.(1), where the integration now is over the 3D sphere around the Weyl point in the $3+1$ space (p_0, p_x, p_y, p_z)[9]. In the vicinity of these points the fermionic quasiparticles behave as chiral (left-handed and right-handed) Weyl fermions in particle physics. That is why such nodes are called the Weyl points. Arrows in Fig. (7) show the direction of the effective spin of the Weyl fermion. This spin is parallel to $\mathbf{p} - \mathbf{p}_+$ in the vicinity of $\mathbf{p}_+$, which means that the fermions living there are right-handed. For the left-handed fermions near $\mathbf{p}_-$, their effective spin is anti-parallel to $\mathbf{p} - \mathbf{p}_-$.

According to the bulk-surface correspondence, at each p_z, for which $N(p_z) = 1$, there should be one branch of Andreev-Majorana edge states which cross zero energy level, see Fig. 2. As a result one has the line of zero energy states in the range $-p_F < p_z < p_F$. This line represents the Fermi surface (Fermi line) in the two-dimensional momentum space of bound states. As the conventional Fermi surface, it separates the positive and negative energy levels But as distinct from the conventional Fermi surface, this Fermi surface is not closed. It has two end points, and this is the reason why this line is called the Fermi arc.

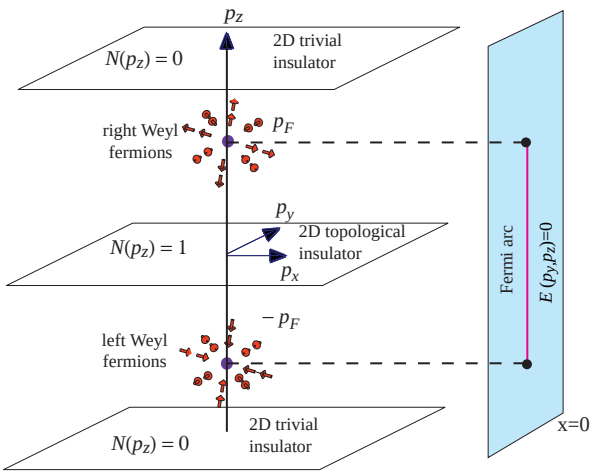

FIG. 7: Line of Andreev-Majorana bound states on surface of chiral superfluid with Weyl points. This line represents the 1D Fermi surface, which separates the edge states with positive and negative energies (see also Fig. 9). However, as distinct from conventional Fermi surfaces, this Fermi surface has end points, and thus is called the The end points of the Fermi arc are determined by projections of the bulk Weyl points to the surface.

The end points of the Fermi arc coincide with the projection of the Weyl points to the surface. This is the consequence of bulk surface correspondence in the Weyl systems[25]. For the arbitrary direction of the surface with the angle λ between the normal to the surface and the axis z, the Fermi arc is concentrated in the range of momenta $-p_F \sin\lambda < p_z < p_F \sin\lambda$. Note that in ^{3}He-A the boundary conditions require $\lambda = 0$.

In crystals, the Weyl points can be moved to the boundaries of the Brillouin zone, where they annihilate each other. As a result one obtains the chiral $3+1$ topological insulator or the fully gapped chiral topological superconductor. Since $N(p_z) = 1$ for all p_z the topological Fermi arc on the boundaries, transforms to the closed topological Fermi surface.

B. Andreev-Majorana Fermi arcs on soliton and domain wall

The similar Fermi arcs appear on the domain walls or solitons separating the chiral phases with opposite chiralities. One has $N(|p_z| < p_F) = +1$ on one side of the soliton/wall and $N(|p_z| < p_F) = -1$ on the other side. According to the index theorem[9,44], the difference between these two values determines the number of the zero modes at the interface between the 2+1 topological insulators for each $|p_z| < p_F$. As a result the domain wall and soliton contain two Fermi arcs instead of single Fermi arc on boundary, see Fig. 8.

Fermi arc on the domain walls in ^{3}He-A[70] has been considered in Refs. 27,71.

Fig. 9 includes also the bound states with non-zero energy and demonstrates that the Fermi arc does represent the piece of the Fermi surface, which separates the positive and negative energy levels.

V. TOPOLOGICAL SUPERFLUIDS WITH LINES OF ZEROES. AM SURFACE FLAT BAND.

The zero-dimensional point nodes in bulk (the Weyl points) give rise to the one-dimensional nodes (lines) in the spectrum of AMBS. In the same manner, the 1D nodal lines in bulk give rise to the 2D manifolds of AM bound states with zero energy, see Fig. **??**. Let us consider the topological origin of such dispersionless spectrum – the flat band – on example of the polar phase of triplet superfluid/superconductor[32].

A. Flat band of AM modes on surface of polar phase

The Hamiltonian for the polar phase is

$$H = \left(\frac{p^2}{2m} - \mu\right)\tau_3 - c\tau_1\sigma_z p_z \,. \qquad (15)$$

This superconductor obeys the time reversal and space inversion symmetry, and it has a line of zeroes in the form of a ring.

For simplicity we consider the spinless fermions, or which is the same, the fully spin polarized fermions, whose Hamiltonain is

$$H = \left(\frac{p^2}{2m} - \mu\right)\tau_3 - c\tau_1 p_z \,. \qquad (16)$$

The spectrum of such fermions has the nodal line – the ring $p_x^2 + p_y^2 = p_F^2$, $p_z = 0$. The stability of this nodal line is determined by the topological invariant protected by symmetry

$$N_K = \frac{1}{4\pi i}\ \mathrm{tr}\ K \oint_C dl\ H^{-1}\nabla_l H \,. \qquad (17)$$

Here the integral is along the loop C around the nodal line in momentum space, see Fig. 11; and the matrix $K = \tau_2$ anticommutes with the Hamiltonian. The winding number around the element of the nodal line is $N_K = 1$.

Now let us consider the momentum $\mathbf{p}_\perp$ as a parameter of the $1+1$ system, then for $|\mathbf{p}_\perp| \neq p_F$ the system represents the fully gapped state – the $1+1$ insulators. This insulator can be described by the same invariant as in Eq.(17) with the contour of integration chosen parallel to p_z. Since at $p_z \to \pm\infty$ the Hamiltonian tends to the same limit, points $p_z = \pm\infty$ are equivalent, and the line $-\infty < p_z < \infty$ forms the closed loop. That is why the integral

$$N_K(\mathbf{p}_\perp) = \frac{1}{4\pi i}\ \mathrm{tr}\ K \int_{-\infty}^{+\infty} dp_z\ H^{-1}\nabla_{p_z} H \,, \qquad (18)$$

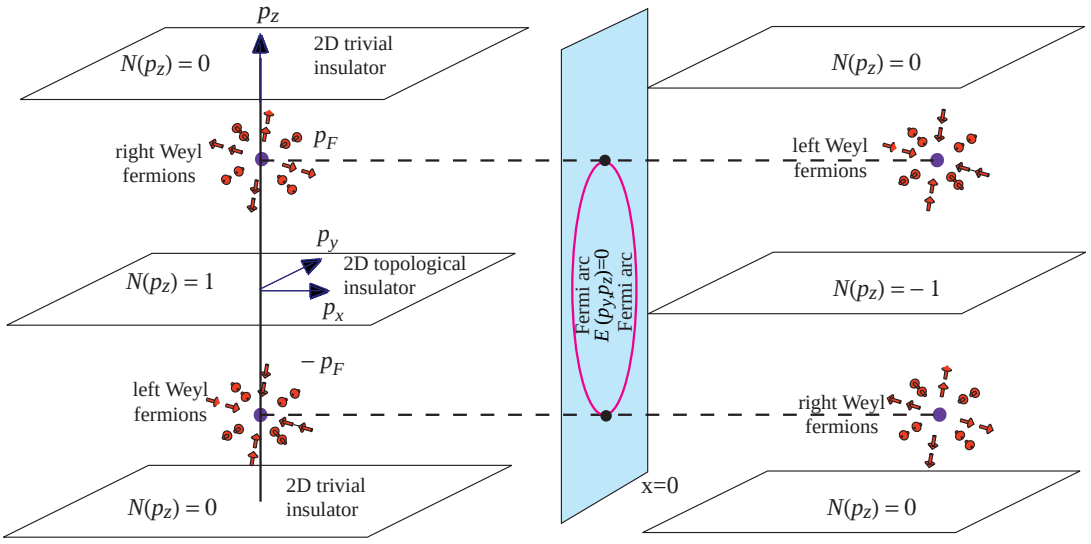

FIG. 8: Topology of Andreev bound states on $\hat{\mathbf{l}}$ soliton[69]. Momentum space topology of Weyl points in bulk ^{3}He-A on two sides of the soliton prescribes existence of Fermi arcs in the spectrum of the Andreev bound states in the soliton or at the interface between the bulk states with different positions of Weyl points. In the considered case the Weyl points on two sides of the interface have the same positions in momentum space, but the opposite chiralities. As a result, the $2+1$ topological insulators have opposite topological invariants. $N(p_z = 0) = \pm 1$. This leads to two Fermi arcs terminating on the projections of the Weyl points on the soliton/interface plane according to the index theorem $n(\text{right}) - n(\text{left}) = 2$.

.

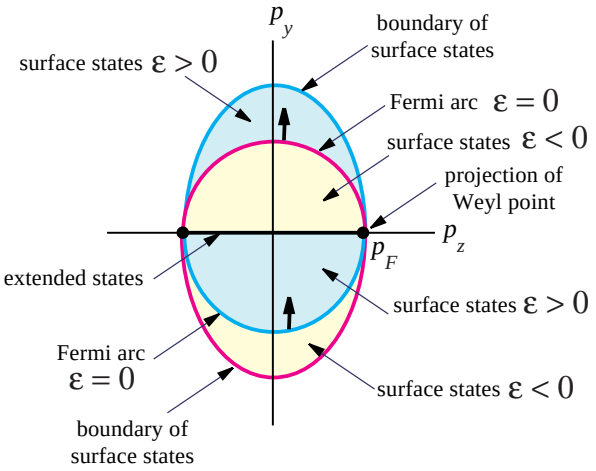

FIG. 9: The spectrum of bound states with two Fermi arcs $\epsilon(p_y, p_z) = 0$. Thick arrows show directions of Fermi velocity at these Fermi arcs. At $p_z = 0$ the velocity is in the same direction, $v_y > 0$, which demonstrates that both Fermi arcs have the same topological charge $N = +1$, which together satisfy the index theorem $n(\text{right}) - n(\text{left}) = 2$, in agreement with momentum space topology of Weyl points in bulk ^{3}He-A on two sides of the soliton in Fig. 8. This leads to discontinuity in the spectrum of bound states at $p_y = 0$, where the spectrum merges with the bulk spectrum.

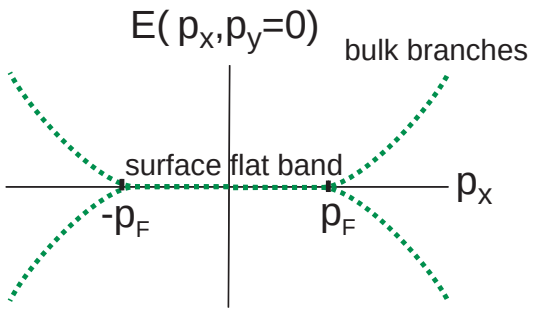

FIG. 10: Spectrum of AM modes on the surface of polar phase. These modes form the 2D flat band: all the states with $p_x^2 + p_y^2 < p_F^2$ have zero energy. The spectrum is shown for $p_y = 0$.

is integer-valued.

Topological invariant $N(\mathbf{p}_\perp)$ in (18) determines the property of the surface bound states of the $1+1$ system at each $\mathbf{p}_\perp$. Due to the bulk-edge correspondence, the topological 1D insulator must have the surface state with exactly zero energy. Since such states exist for any parameter within the circle $|\mathbf{p}_\perp| = p_F$, one obtains the flat band of AM modes in Fig. 11 *left* – the continuum of the self conjugate bound states with exactly zero energy, $E(|\mathbf{p}_\perp| < p_F) = 0$, which are protected by topology. Such modes do not exist for parameters $|\mathbf{p}_\perp| > p_F$, for which the $1+1$ superfluid is non-topological.

In a spinful polar phase with the Hamiltonian (15) the nodal ring in bulk gives rise to two surface flat bands with opposite chiralities for two directions of spin. The tiny spin-orbit interaction leads to a small splitting of the

Andreev-Majorana modes.

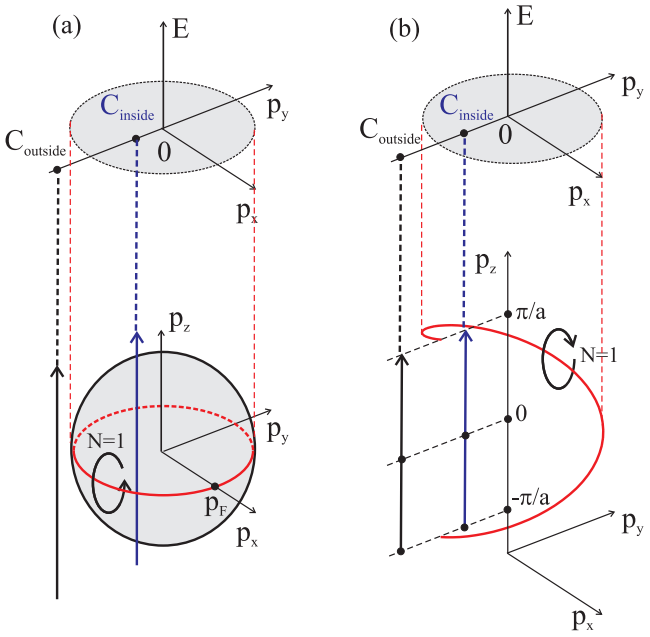

FIG. 11: Topologically nontrivial nodal lines generate topologically protected flat bands on the surface: (a) closed equatorial line of zeroes in the polar phase; (b) spiral of zeroes in the multilayered graphene is also the closed line. Projection of the line on the surface determines boundary of flat band. Let us fix (p_x, p_y). If for a given (p_x, p_y) the energy $E(p_x, p_y, p_z)$ is nonzero for any p_z, then the Green's function $G(\omega, p_z)_{p_x,p_y}$ describes the 1D fully gapped system – "insulator". At each (p_x, p_y) inside the projection of the line to the surface, this insulator is topological, since it is described by non-zero topological invariant (18). Thus for such (p_x, p_y) there is the gapless edge state on the surface. The manifold of these zero-energy edge state inside the projection forms the flat band.

B. Flat band on surface of model graphite

In the multilayered graphene, when the number of the graphene layers tends to infinity, and if some small matrix elements are neglected, the formed $3+1$ system has line of zeroes, which also obeys the invariant similar to that in Eq.(17). This nodal line has a shape of a spiral[32,33], see Fig. 11.

Let us again consider the momentum $\mathbf{p}_\perp$ as a parameter of the $1+1$ system, then for $|\mathbf{p}_\perp| \neq t$, where t is the dominating hopping element, the system represents the fully gapped system – the $1+1$ insulators. This insulator can be described by the same invariant as in Eq.(17) with the contour of integration chosen parallel to p_z, i.e. along the 1D Brillouin zone at fixed $\mathbf{p}_\perp$. Due to periodic boundary conditions, the points $p_z = \pm\pi/a$, where a is the distance between the layers, are equivalent and the contour of integrations forms the closed loop. As a result one obtains the integer valued invariant

$$N_K(\mathbf{p}_\perp) = \frac{1}{4\pi i}\ \mathrm{tr}\ \int_{-\pi/a}^{+\pi/a} dp_z\ \tau_2 H^{-1}\nabla_{p_z} H\,. \qquad (19)$$

For $|\mathbf{p}_\perp| < t$ the $1+1$ insulator is topological, since $N(|\mathbf{p}_\perp| < t) = 1$. This gives rise to the surface flat band. Since there are no Cooper pair correlations, the fermionic bound states within the flat band are not the Majorana modes.

VI. AM MODES ON VORTICES IN CHIRAL $2+1$ SUPERFLUIDS

The low-energy fermions bound to the vortex core play the main role in the thermodynamics and dynamics of the vortex state in superconductors and Fermi-superfluids. The spectrum of the low-energy bound states in the core of the axisymmetric vortex with winding number $\nu = \pm 1$ was obtained by Caroli, de Gennes and Matricon for the isotropic model of s-wave superconductor in the weak coupling limit, $\Delta \ll \mu$:[72]:

$$E_n(p_z) = -\nu\omega_0(p_z)\left(n + \frac{1}{2}\right)\ , \qquad (20)$$

This spectrum is two-fold degenerate due to spin degrees of freedom. The integral number n is the quantum number related to the angular momentum of the bound state fermions. The minigap – the level spacing $\omega_0(p_z)$ – corresponds to the angular velocity of the fermionic quasiparticle orbiting about the vortex axis. The direction of rotation is determined by the sign of the winding number ν of the vortex.

The level spacing is typically small compared to the energy gap of the quasiparticles outside the core, $\omega_0 \sim \Delta^2/\mu \ll \Delta$. So, in many physical cases the discreteness of n can be neglected. In such cases the spectrum crosses zero energy as a function of continuous angular momentum L_z, and one may consider this as spectrum of quasi zero modes. The fermions in this 1D "Fermi liquid" are chiral: the positive energy fermions have a definite sign of the angular momentum L_z. The number of the branches crossing zero energy as function of continuous L_z obeys the index theorem[9].

Here we are interested in the fine structure of the spectrum, when its discrete nature is important. This takes place for example in the ultracold fermionic gases near the Feshbach resonance, when Δ is not small.

Let us first consider the $2+1$ space-time and start with the weak coupling limit. The Majorana nature of the Bogoliubov particles requires that the spectrum must be symmetric with respect to zero energy, i.e. for each level with energy E there must be the level with the energy $-E$. For fermions on vortices such condition is satisfied for two classes of systems. In the systems on the first class the spectrum of Andreev bound states $E_n = \omega_0(n + 1/2)$. Vortices in s-wave superconductors belong

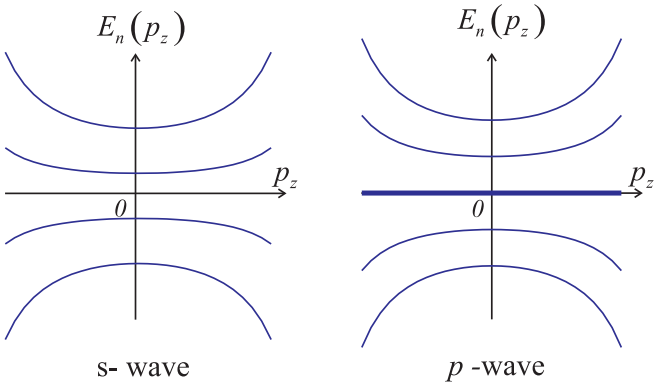

FIG. 12: *left* : Schematic illustration of spectrum of the fermionic bound states in the core of $\nu = 1$ vortex in s-wave superconductor. In the weak coupling limit the lowest branches are equidistant: $E_n(p_z) = -\omega_0(p_z)\left(n + \frac{1}{2}\right)$. There are no zero energy states. The spectrum is doubly degenerate over spin. *right* : The spectrum of bound states in the most symmetric vortices in the p-wave superfluids: the ciral Weyl superfluid ^{3}He-A and the time reversal invariant planar phase. The spectrum is $E_n(p_z) = -\omega_0(p_z)n$. The branch with $n = 0$ forms the flat band of Andreev-Majorana modes.

to this class. Vortices of the second class have $E_n = \omega_0 n$. They contain the Andreev-Majorana mode with exactly zero energy level at $n = 0$. In the $2+1$ system this mode is not propagating and is self-conjugated. That is why it is called the Majorana mode instead of the Majorana particle (see Ref.[21]).

Let us for simplicity consider the spinless (or fully spin polarized) chiral $p_x + ip_y$ superfluid in $2 + 1$ space-time, which is described by Eq.(3). As it was shown in Ref.[23] the vortices with winding number $\nu = 1$ or $\nu = -1$ belong to the second class:

$$E_n = -\nu\omega_0 n\,, \tag{21}$$

and thus contain a single Majorana mode at $n = 0$. This mode is robust to perturbations, since it is self-conjugated and thus must obey the condition $E = -E$, see also[73].

For the spinful fermions in Eq.(2) there are two AM modes corresponding to the two spin projections. The even number of Majorana modes is not robust to perturbations. For example, the spin-orbit interaction splits two modes with $E_1 = -E_2$. The splitting is absent, if there is some discrete symmetry between the AM modes, such as the mirror symmetry in Ref.[74].

In the spinful $p_x + ip_y$ there is a topological object, which carries a single Majorana mode. It is the half-quantum vortex[75]. In a simple model, the half-quantum vortex is the vortex with $\nu_\uparrow = 1$ in one spin component, while the other spin component has zero vorticity $\nu_\downarrow = 0$. As a result such vortex contains single Majorana mode, which is robust to perturbations.

However, the perturbations should not be too large. In the limit when μ is negative and large, the BCS is transformed to the BEC of molecules, where the Majorana mode is absent. The Majorana mode disappears, when the chemical potential μ crosses zero. At $\mu = 0$ there is a topological quantum phase transition (TQPT), at which the topological invariant in Eq.(1) changes from $N = 1$ to $N = 0$. The topological transition cannot occur adiabatically, and in the intermediate state with $\mu = 0$, the spectrum in bulk becomes gapless. At $\mu = 0$ the Majorana mode merges with the continuous spectrum of bulk quasiparticles and disappears at $\mu < 0$. This demonstrates the topological origin of the AM mode, which exists inside the vortex only if the vacuum in bulk is topologically nontrivial.

VII. AM FLAT BAND IN A VORTEX IN WEYL SUPERFLUIDS

One can easily extend the consideration in Sec. VI to the $3 + 1$ case in the weak coupling limit. The levels at $p_z \neq 0$ remain equidistant according to the Caroli-de Gennes-Matricon solution and they must be symmetric with respect to $E = 0$. This dictates the following modification of Eq.(20) for the most symmetric vortices in ^{3}He-A and in the planar phase:

$$E_n(p_z) = -\nu\omega_0(p_z)n\,. \tag{22}$$

This equation suggests the flat band in the vortex core for $n = 0$, see Fig. 12 *right*. Now we show how such flat band emerges purely from the topological considerations, which do not use the weak coupling approximation.

Topology of bound states on vortices in $3 + 1$ chiral superfluids can be obtained by dimensional extension of the topology in the $2+1$ case. The AM mode in the point vortex of fully gapped $2 + 1$ chiral superfluid transforms to the flat band of AM modes inside the vortex line in $3 + 1$ chiral superfluids with Weyl points in bulk. Let us consider again the p_x+ip_y state in Eq.(13), and choose for a moment the direction of the vortex line along the axis z. In this case p_z is the quantum number of the bound states in the vortex core. For each p_z in the range $-p_F < p_z < p_F$ the Green's function (13) describes the $2 + 1$ chiral superfluid with topological invariant $N(|p_z| < p_F) = 1$ in Eq.(14), and this superfluid contains the point vortex. The point vortex in the $2 + 1$ topologically nontrivial chiral superfluid contains the AM mode with zero energy. The continuum of the Andreev-Majorana modes in the range $-p_F < p_z < p_F$ forms the flat band.

This is demonstrated in Fig. (13), in which the vortex axis is rotated by angle λ with respect to the direction to the Wey points. In this case the invariant (14)

$$N(p_z) = 1 \quad , \quad |p_z| < p_F|\cos\lambda|\,, \tag{23}$$
$$N(p_z) = 0 \quad , \quad |p_z| > p_F|\cos\lambda|\,. \tag{24}$$

Such flat band of AM modes has been predicted by Kopnin and Salomaa in Ref. 28 for the $\nu = 1$ vortex in

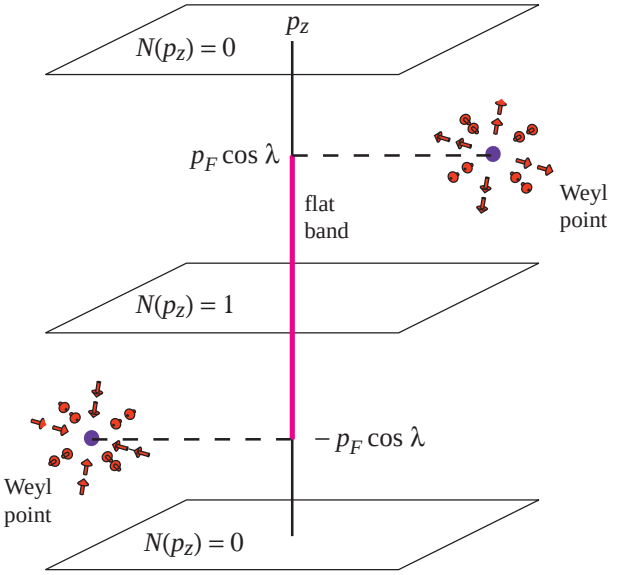

FIG. 13: Projections of Weyl points on the direction of the vortex axis (the z-axis) determine the boundaries of the flat band in the vortex core. Weyl point in 3D systems represents the hedgehog (Berry phase monopole) in momentum space[9]. For each plane $p_z = \text{const}$ one has the effective 2D system with the fully gapped energy spectrum $E_{p_z}(p_x, p_y)$, except for the planes with $p_{z\pm} = \pm p_F \cos\lambda$, where the energy $E_{p_z}(p_x, p_y)$ has a node due to the presence of the hedgehogs in these planes. Topological invariant $N(p_z)$ in (14) is non-zero for $|p_z| < p_F|\cos\lambda|$, which means that for any value of the parameter p_z in this interval the system behaves as a 2D topological insulator or 2D fully gapped topological superfluid. Point vortex in such 2D superfluids has fermionic state with exactly zero energy. For the vortex line in the original 3D system with Fermi points this corresponds to the dispersionless spectrum of fermion zero modes in the whole interval $|p_z| < p_F|\cos\lambda|$ (thick line).

^{3}He-A. This flat band is doubly degenerate over spin and thus it may split, for example, due to spin-orbit interaction (the non-degenerate flat band of Andreev-Majorana fermions takes place in the core of half-quantum vortex). In superfluid ^{3}He the spin-orbit interaction is very small and can be neglected. However, there can be another source of splitting: the symmetry of the vortex core can be spontaneously broken (see[75]).

The same doubly degenerate flat band should exist in the $\nu = 1$ vortex in the $3 + 1$ planar phase, where the Green's function is

$$G^{-1} = ip_0 + \tau_3 \left(\frac{p^2}{2m} - \mu \right) + \tau_1(\sigma_x p_x + \sigma_y p_y) \,. \quad (25)$$

Here now $p^2 = p_x^2 + p_y^2 + p_z^2$. For the $3 + 1$ planar phase, the topological invariant N_K in (6) is extended to:

$$N_K(p_z) = \\ = \frac{1}{4\pi^2} \, \mathbf{tr} \left[K \int dp_x dp_y dp_0 \; G\partial_{p_x} G^{-1} G\partial_{p_y} G^{-1} G\partial_{p_0} G^{-1} \right], \quad (26)$$

giving $N_K(|p_z| < p_F \cos\lambda) = 2$.

Both flat bands, in the A-phase and in the planar phase, appear only for $\mu > 0$, when $N_K(p_z = 0) = 2$. For $\mu < 0$ the superfluids are topologically trivial, $N_K(p_z = 0) = 0$, and the flat band does not exist.

VIII. AMBS IN ^{3} HE-B VORTEX

A. From planar phase to B-phase

Dimensional extension of the $2+1$ planar phase allows to understand the topological properties of the vortex spectrum in ^{3}He-B. The Hamiltonian (9) for fermions in the bulk ^{3}He-B represents at $p_z = 0$ the $2 + 1$ planar phase. That is why at $p_z = 0$ the $\nu = 1$ vortex in ^{3}He-B contains two AM bound states with zero energy, if the tiny spin-orbit interaction is neglected and the core symmetry is not spontaneously broken. For $p_z \neq 0$ the zero energy modes are not supported by topology. So the two branches of AM modes split, and one may expect the behavior of the spectrum of AM bound states in the most symmetric vortex as illustrated in Fig. 15a,b.

For ^{3}He-B, which lives in the range of parameters where $N^K \neq 0$ in Fig. 15a, the gapless fermions in the core of the most symmetric vortex (the so-called o-vortex[75]) have been found in Ref.[76]. On the other hand, in the BEC limit, when μ is negative and the Bose condensate of molecules takes place, there are no gapless fermions, see Fig. 15b. Thus in the BCS-BEC crossover region the spectrum of fermions localized on vortices must be reconstructed. The topological reconstruction of the fermionic spectrum in the vortex core cannot occur adiabatically. It should occur only during the topological quantum phase transition in bulk, when the bulk gapless state is crossed. Such topological transition occurs at $\mu = 0$, see Fig. 4. At $\mu < 0$ the topological charge N^K nullifies and simultaneously the gap in the spectrum of core fermions arises, see Fig. 15b.

This again demonstrates that the existence of fermion zero modes is closely related to the topological properties of the vacuum state. The reconstruction of the spectrum of fermion zero modes at the TQPT in bulk can be also seen for vortices in relativistic superconductors[77].

B. AMBS on B-phase vortices with broken symmetry

The spectrum in Fig. 15 *left* is valid only for the vortex state, which respects all the possible symmetries of the vortex core. These symmetries are the space parity P and the discrete symmetry TU_2. The latter is the symmetry under the time reversal T when it is accompanied by the π-rotation U_2 about the axis perpendicular to the vortex axis. In the cores of the experimentally observed vortices in ^{3}He-B both discrete symmetries are spontaneously broken, while the combined symmetry PTU_2 is

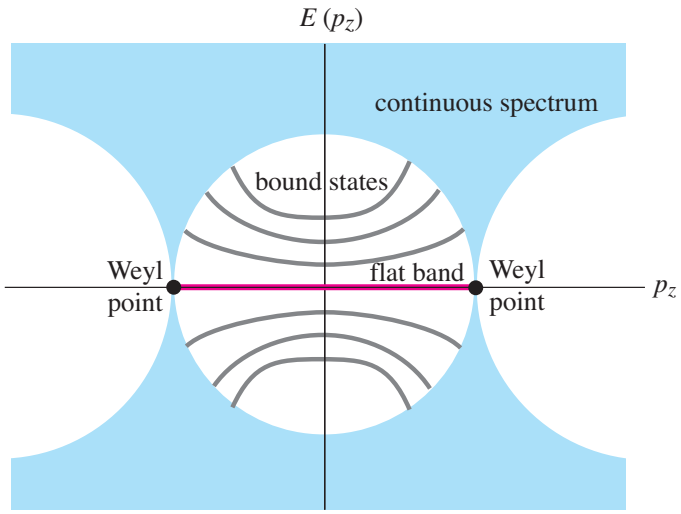

FIG. 14: Schematic illustration of the spectrum of bound states $E(p_z)$ in the vortex core of Weyl superfluid. The branches of bound states terminate at points where their spectrum merges with the continuous spectrum in the bulk. The flat band terminates at points where the spectrum has zeroes in the bulk, i.e. when it merges with Weyl points. It is the **p**-space analog of a Dirac string terminating on a monopole, another analog is given by the Fermi arc in Fig. 1 *bottom right* .

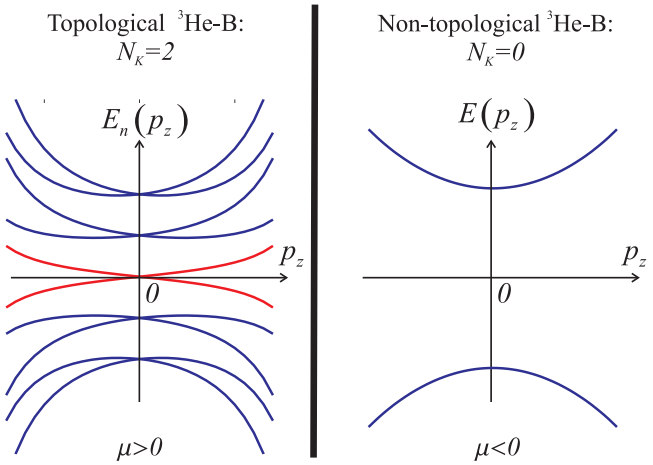

FIG. 15: (*a*) Schematic illustration of spectrum of the fermionic bound states in the core of the of the most symmetric vortex (*o*-vortex) in ^{3}He-B. Two AM states with zero energy exist at $p_z = 0$. (*b*): The same vortex but in the topologically trivial state of the liquid, $N_K = 0$, does not have fermion zero modes. The spectrum of bound states is fully gapped. Fermion zero modes disappear at the topological quantum phase transition, which occurs in bulk liquid at $\mu = 0$. Similar situation may take place for strings in color superconductors in quark matter[77].

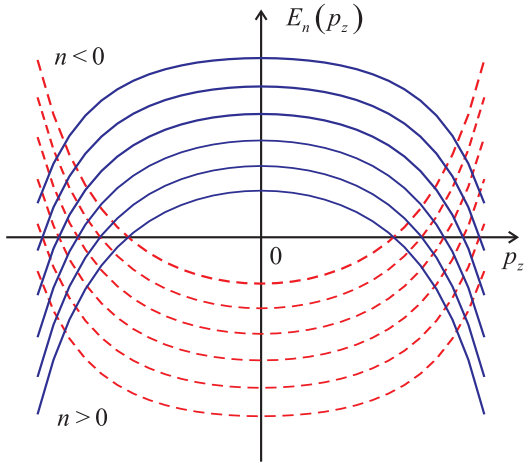

FIG. 16: Spectrum of AMBS in the axisymmetric v-vortex with spontaneously broken discrete symmetry in ^{3}He-B. The AM states with zero energy at $p_z = 0$, which were present in the most symmetric *o*-vortex in Fig. 15, do not exist any more. They split due to matrix element between the spin components, which appears due to symmetry breaking and move far away. There are many non-topological branches of spectrum, which cross zero energy as function of p_z and form the one-dimensional Fermi surfaces. The number of such branches $\sim \sqrt{\mu/mc^2}$.

preserved[75]. Such vortex is called the v-vortex. The broken parity in the v-vortex leads to mixing between the two spin components in the core, as a result the two AM modes at $p_z = 0$ split. This leads to the following spectrum in Fig. 16[78].

In the weak coupling regime, $mc^2 \ll \mu$, there appear the large number (on the order of $\sqrt{\mu/mc^2}$) of branches, which cross zero energy. Each crossing point corresponds to the one-dimensional Fermi-surface. This demonstrates that the topology in bulk determines the spectrum of the fermion zero modes on the B-phase vortices only if

the symmetry of the vortex core is not violated. This is the consequence of the mod 2 rule for Majorana modes: the topological zero energy state survives the symmetry breaking only in case of the odd number of Majorana modes. So, for the realistic vortices the AM mode can exist only in half-quantum vortices. For the other vortices, such as in ^{3}He-B, the large number of the energy levels is nvolved. That is why for the consideration it is more appropriate to use the quasiclassical approximation. The latter leads to the other types of topological invariants describing the fermion zero modes on vortices, see e.g. Refs. 9,79.

IX. CONCLUSION

We considered the Andreev-Majorana bound states with zero energy on surfaces, interfaces and vortices in different phases of the p-wave superfluids: ^{3}He-A, ^{3}He-B, planar and polar phases.

These states are determined by topology in bulk, and they disappear at the quantum phase transition from the topological to non-topological state of the superfluid (see example in Fig. 15). This topology demonstrates the interplay of dimensions. In particular, the 0D Weyl point (the Berry phase monopole in momentum space) gives rise to the 1D Fermi arc on the surface (Sec. IV A). The 1D nodal line in bulk produces the dispersional 2D band of AM modes on the surface (Sec. V).

The interplay of dimensions also connects the AM states in superfluids in different dimensions. For example, the property of the spectrum of bound states in the 3D ^{3}He-B is connected to the property of the spectrum in the 2D planar phase (see Sec. III for edge states and Sec. VIII A for bound states on vortices). The 0D AM mode on a point vortex in 2D chiral superfluid (Sec. VI) gives rise to the 1D flat band of AM modes on a vortex in the 3D chiral superfluid (Sec. VII).

The most robust zero energy edge states take place on the boundary of ^{3}He-A, or in general on boundaries and interfaces of chiral superfluids with the topological invariant N in Eq.(1). In the other phases, the existence zero energy edge states is supported by symmetry, i.e. by the symmetry protected topological invariants N_K in Eqs. (6) and (17). When the symmetry is violated in bulk or on the boundary/interface, the AM bound states acquire gap.

Concerning the AM states on vortices, only the states on half quantum vortices are fully robust to perturbations. In the singly quantized vortices the fate of zero energy states depend on symmetry and its possible violation in bulk or spontaneous breaking inside the vortex core. This the consequence of the Z_2 classification of the AM modes on vortices. On the other hand, the spontaneously broken symmetry inside the vortex core may give rise to many non-topological branches of AMBS, which cross zero energy as function of p_z. This is demonstrated in Sec. VIII B.

Let us also mention the application to the relativistic theories. The fermion zero modes obtained in the Dirac systems, such as the modes localized on strings in Ref.[80], are not properly supported by topology. The reason for that is that the Dirac vacuum is marginal, and the topological invariants depend on the regularization of the Green's function in the ultraviolet[81]. For example, in Fig.4 the Dirac vacuum is on the border between the trivial vacuum with $N_K = 0$ and the topological vacuum with $N_K = 2$. That is why the existence of the modes with exactly zero energy depends on the behavior of the Green's function at infinity.

X. ACKNOWLEDGEMENTS

MS and GEV acknowledge financial support by the Academy of Finland through its LTQ CoE grant (project #250280).

[1] C.W.J. Beenakker, Annihilation of colliding Bogoliubov quasiparticles reveals their Majorana nature, Phys. Rev. Lett. **112**, 070604 (2014).
[2] C. Chamon, R. Jackiw, Y. Nishida, S.-Y. Pi, L. Santos Quantizing Majorana fermions in a superconductor, Phys. Rev. B **81**, 224515 (2010).
[3] T. Senthil, M.P.A. Fisher, Quasiparticle localization in superconductors with spin-orbit scattering, Phys. Rev. B **61**, 9690-9698 (2000).
[4] G.E. Volovik and M.A. Zubkov, Emergent Weyl spinors in multi-fermion systems, Nuclear Physics B **881**, 514–538 (2014), arXiv:1402.5700.
[5] A.P. Schnyder, S. Ryu, A. Furusaki and A.W.W. Ludwig, Classification of topological insulators and superconductors in three spatial dimensions, Phys. Rev. **B 78**, 195125 (2008).
[6] A.P. Schnyder, S. Ryu, A. Furusaki and A.W.W. Ludwig, Classification of topological insulators and superconductors, AIP Conf. Proc. **1134**, 10 (2009); arXiv:0905.2029.
[7] A.P. Schnyder, S. Ryu and A.W.W. Ludwig, Lattice model of three-dimensional topological singlet superconductor with time-reversal symmetry Phys. Rev. Lett. **102**, 196804 (2009); arXiv:0901.1343.
[8] A. Kitaev, Periodic table for topological insulators and superconductors, AIP Conference Proceedings, Volume **1134**, pp. 22-30 (2009); arXiv:0901.2686.
[9] G.E. Volovik, *The Universe in a Helium Droplet*, Clarendon Press, Oxford (2003).
[10] G.E. Volovik, Quantum phase transitions from topology in momentum space, in: "Quantum Analogues: From Phase Transitions to Black Holes and Cosmology", eds. W.G. Unruh and R. Schützhold, Springer Lecture Notes in Physics **718** (2007), pp. 31–73; cond-mat/0601372.
[11] P. Hořava, Stability of Fermi surfaces and K-theory, Phys.

Rev. Lett. **95**, 016405 (2005).
[12] M.Z. Hasan and C.L. Kane, Topological Insulators, Rev. Mod. Phys. **82**, 3045 (2010).
[13] Xiao-Liang Qi and Shou-Cheng Zhang, Topological insulators and superconductors, Rev. Mod. Phys. **83**, 1057–1110 (2011).
[14] M.A. Silaev and G.E. Volovik, Topological superfluid ^{3}He-B: fermion zero modes on interfaces and in the vortex core, J. Low Temp. Phys. **161**, 460–473 (2010); arXiv:1005.4672.
[15] G.E. Volovik, On edge states in superconductor with time inversion symmetry breaking, Pis'ma ZhETF **66**, 492–497 (1997); JETP Lett. **66**, 522–527 (1997), arXiv:cond-mat/9709084.
[16] Suk Bum Chung, Shou-Cheng Zhang, Detecting the Majorana fermion surface state of ^{3}He-B through spin relaxation, Phys. Rev. Lett. **103**, 235301 (2009); arXiv:0907.4394.
[17] G.E. Volovik, Fermion zero modes at the boundary of superfluid ^{3}He-B, Pis'ma ZhETF **90**, 440–442 (2009); JETP Lett. **90**, 398–401 (2009); arXiv:0907.5389.
[18] Y. Nagato, S. Higashitani and K. Nagai, Strong anisotropy in spin suceptibility of superfluid He-3-B film caused by surface bound states, J. Phys. Soc. Japan **78**, 123603 (2009).
[19] M.M. Salomaa and G.E. Volovik, Cosmiclike domain walls in superfluid ^{3}He-B: Instantons and diabolical points in (**k**, **r**) space, Phys. Rev. **B 37**, 9298–9311 (1988).
[20] G.E. Volovik, Topological invariant for superfluid ^{3}He-B and quantum phase transitions, Pis'ma ZhETF **90**, 639–643 (2009); JETP Lett. **90**, 587–591 (2009); arXiv:0909.3084.
[21] F. Wilczek, Emergent Majorana mass and axion couplings in superfluids, arXiv:1401.4379.
[22] D. A. Ivanov, Non-Abelian statistics of half-quantum vortices in p- wave superconductors, Phys. Rev. Lett. **86**, 268-271 (2001).
[23] G.E. Volovik, Fermion zero modes on vortices in chiral superconductors, Pis'ma ZhETF **70**, 601–606 (1999); JETP Lett. **70**, 609-614 (1999); cond-mat/9909426.
[24] Y. Tsutsumi, M. Ichioka and K. Machida, Majorana surface states of superfluid ^{3}He-A and B phases in a slab, Phys. Rev. B **83**, 094510 (2011).
[25] Xiangang Wan, A.M. Turner, A. Vishwanath and S.Y. Savrasov, Topological semimetal and Fermi-arc surface states in the electronic structure of pyrochlore iridates, Phys. Rev. B **83**, 205101 (2011).
[26] A.A. Burkov and L. Balents, Weyl semimetal in a topological insulator multilayer, Phys. Rev. Lett. **107**, 127205 (2011).
[27] M.A. Silaev and G.E. Volovik, Topological Fermi arcs in superfluid ^{3}He, Phys. Rev. B **86**, 214511(2012); arXiv:1209.3368.
[28] N.B. Kopnin, and M.M. Salomaa, Phys. Rev. **B 44**, 9667 (1991).
[29] Y. Tanaka and S. Kashiwaya, Theory of tunneling spectroscopy of d-wave superconductors, Phys. Rev. Lett. **74**, 3451–3454 (1995).
[30] S. Ryu and Y. Hatsugai, Topological origin of zero-energy edge states in particle-hole symmetric systems, Phys. Rev. Lett. **89**, 077002 (2002).
[31] A.P. Schnyder and S. Ryu, Topological phases and flat surface bands in superconductors without inversion symmetry, arXiv:1011.1438; Phys. Rev. B **84**, 060504(R) (2011).
[32] T.T. Heikkilä and G.E. Volovik, Dimensional crossover in topological matter: Evolution of the multiple Dirac point in the layered system to the flat band on the surface, Pis'ma ZhETF **93**, 63–68 (2011); JETP Lett. **93**, 59–65 (2011); arXiv:1011.4185.
[33] T.T. Heikkilä, N.B. Kopnin and G.E. Volovik, Flat bands in topological media, Pis'ma ZhETF **94**, 252– 258 (2011); JETP Lett. **94**, 233–239(2011); arXiv:1012.0905.
[34] G.E. Volovik, Flat band in the core of topological defects: bulk-vortex correspondence in topological superfluids with Fermi points, Pis'ma ZhETF **93**, 69–72 (2011); JETP Lett. **93**, 66–69 (2011); arXiv:1011.4665.
[35] M. Sato, Y. Tanaka, K. Yada and T. Yokoyama, Topology of Andreev bound states with flat dispersion, Phys. Rev. B **83**, 224511 (2011).
[36] L. V. Levitin, R. G. Bennett, A. Casey, B. Cowan, J. Saunders, D. Drung, Th. Schurig, J. M. Parpia, B. Ilic, N. Zhelev, Study of Superfluid ^{3}He under nanoscale confinement: A new approach to the investigation of superfluid ^{3}He films, J. Low Temp. Phys. **175**, 667–680 (2014).
[37] H. So, Induced topological invariants by lattice fermions in odd dimensions, Prog. Theor. Phys. **74**, 585–593 (1985).
[38] K. Ishikawa and T. Matsuyama, Magnetic field induced multi component QED in three-dimensions and quantum Hall effect, Z. Phys. C **33**, 41–45 (1986).
[39] K. Ishikawa and T. Matsuyama, A microscopic theory of the quantum Hall effect, Nucl. Phys. **B 280**, 523–548 (1987).
[40] G.E. Volovik, Analog of quantum Hall effect in superfluid ^{3}He film, JETP **67**, 1804–1811 (1988).
[41] G.E. Volovik and V.M. Yakovenko, Fractional charge, spin and statistics of solitons in superfluid ^{3}He film, J. Phys.: Condens. Matter **1**, 5263–5274 (1989).
[42] D. J. Thouless, M. Kohmoto, M. P. Nightingale, and M. den Nijs, Quantized Hall conductance in a two-dimensional periodic potential, Phys. Rev. Lett. **49**, 405 (1982).
[43] Q. Niu, D. J. Thouless, and Y.-Sh. Wu, Quantized Hall conductance as a topological invariant, Phys. Rev. B **31**, 3372 (1985).
[44] G.E. Volovik, Quantum Hall and chiral edge states in thin ^{3}He-A film, JETP Lett. **55**, 368–363 (1992).
[45] D. Vollhardt and P. Woelfe, *The superfluid phases of helium 3*, Taylor & Francis, 1990.
[46] L. Levitin, R. Bennett, A. Casey, B. Cowan, J. Parpia, and L. Saunders, J. Low Temp. Phys. **158**, 163 (2010).
[47] L.V. Levitin and R.G. Bennett and A. Casey and B. Cowan and J. Parpia and L. Saunders, J. Low Temp. Phys., **158**, 159, (2010).
[48] L. Levitin, R. Bennett, A. Casey, B. Cowan, L. Saunders, D. Drung, T. Schurig, and J. Parpia, Science **340**, 841 (2013).
[49] L.V. Levitin, R.G. Bennett, E.V. Surovtsev, J.M. Parpia, B. Cowan, A. J. Casey, and J. Saunders, Phys. Rev. Lett. **111**, 235304 (2013).
[50] G.E. Volovik, *Exotic properties of superfluid ^{3}He*, World Scientific, Singapore, 1992.
[51] G.E. Volovik, Fractional statistics and analogs of quantum Hall effect in superfluid ^{3}He films, AIP Conference Proceedings **194**, 136–146 (1989).
[52] J. A. Sauls, Surface states, edge currents, and the angular momentum of chiral p-wave superfluids, Phys. Rev. B **84**, 214509 (2011).
[53] H. Wu and J. A. Sauls, Majorana excitations, spin and mass currents on the surface of topological superfluid ^{3}He-B, Phys. Rev. B **88**, 184506 (2013).

[54] B.A. Volkov, A.A. Gorbatsevich, Yu.V. Kopaev and V.V. Tugushev, Macroscopic current states in crystals, JETP **54**, 391–397 (1981); B.A. Volkov and O.A. Pankratov, Two-dimensional massless electrons in an inverted contact, JETP Lett. **42**, 178–181 (1985).

[55] K. Nagai, Y.Nagato, M. Yamamoto, S. Higashitani, Surface bound states in superfluid ^{3}He, J. Phys. Soc. Japan, **77**, 111003 (2008).

[56] S. Murakawa, Y. Tamura, Y. Wada, M. Wasai, M. Saitoh, Y. Aoki, R. Nomura, Y. Okuda, Y. Nagato, M. Yamamoto, S. Higashitani, and K. Nagai, New anomaly in the transverse acoustic impedance of superfluid ^{3}He-B with a wall coated by several layers of ^{4}He, Phys. Rev. Lett. **103**, 155301 (2009).

[57] J. P. Davis, J. Pollanen, H. Choi, J. A. Sauls, W. P. Halperin, A. B. Vorontsov, Anomalous attenuation of transverse sound in ^{3}He, Phys. Rev. Lett. **101**, 085301 (2008).

[58] Y. Aoki, Y. Wada, M. Saitoh, R. Nomura, Y. Okuda, Y. Nagato, M. Yamamoto, S. Higashitani, K. Nagai, Observation of surface Andreev bound states of superfluid ^{3}He by transverse acoustic impedance measurements, Phys. Rev. Lett. **95**, 075301 (2005).

[59] H. Choi, J. P. Davis, J. Pollanen, and W. P. Halperin, Surface specific heat of ^{3}He and Andreev bound states, Phys. Rev. Lett. **96**, 125301 (2006).

[60] Y.M. Bunkov, Direct observation of a Majorana quasiparticle heat capacity in ^{3}He, J. Low Temp. Phys. **175**, 385–394 (2014).

[61] Yu. Makhlin, M. Silaev, and G.E. Volovik, Topology of the planar phase of superfluid ^{3}He and bulk-boundary correspondence for three-dimensional topological superconductors, Phys. Rev. B **89** 174502 (2014); arXiv:1312.2677.

[62] M. A. Silaev, G.E. Volovik Evolution of edge states in topological superfluids during the quantum phase transition, JETP Lett.**95**, 25-28 (2012).

[63] V. Gurarie, Single-particle Green's functions and interacting topological insulators, Phys. Rev. B **83**, 085426 (2011).

[64] A.M. Essin and V. Gurarie, Bulk-boundary correspondence of topological insulators from their respective Green's functions, Phys. Rev. B **84**, 125132 (2011).

[65] T. Mizushima, M. Sato, and K. Machida, Symmetry protected topological order and spin susceptibility in superfluid ^{3}He-B, Phys. Rev. Lett. **109**, 165301 (2012).

[66] T. Mizushima, Superfluid ^{3}He in a restricted geometry with a perpendicular magnetic field, Phys. Rev. B **86**, 094518 (2012)

[67] G.E. Volovik, Topological superfluid ^{3}He-B in magnetic field and Ising variable, Pis'ma ZhETF **91**, 215–219 (2010).

[68] L. Fidkowski and A. Kitaev, Effects of interactions on the topological classification of free fermion systems. Phys. Rev. B **81**, 134509 (2010); Topological phases of fermions in one dimension, Phys. Rev. B **83**, 075103 (2011).

[69] T.-L. Ho , J. R. Fulco , J. R Schrieffer and F. Wilczek Solitons in superfluid ^{3}He-A: bound states on domain walls, Phys. Rev. Lett. **52**, 1524–1527 (1984).

[70] M.M. Salomaa, G. E. Volovik, Half-solitons in superfluid ^{3}He-A: Novel $\pi/2$-quanta of phase slippage, J. Low Temp. Phys. **74**, 319-346 (1989).

[71] M. Nakahara, Bound states on domain wall in superfluid 3He -A film, J. Phys. C: Solid State Phys. **19** L195–L199 (1986).

[72] C. Caroli, P.G. de Gennes, and J. Matricon, Bound Fermion states on a vortex line in a type II superconductor, Phys. Lett. **9**, 307–309 (1964).

[73] N. Read and D. Green, Paired states of fermions in two dimensions with breaking of parity and time-reversal symmetries and the fractional quantum Hall effect, Phys. Rev. B **61**, 10267–10297 (2000).

[74] M. Sato, A. Yamakage, and T. Mizushima, Mirror Majorana zero modes in spinful superconductors/superfluids – Non-Abelian anyons in integer quantum vortices, Physica E **55**, 20–24 (2014).

[75] M.M. Salomaa, G.E. Volovik, Quantized vortices in superfluid ^{3}He, Rev. Mod. Phys. **59**, 533–613 (1987).

[76] T. Sh. Misirpashaev and G.E. Volovik, Fermion zero modes in symmetric vortices in superfluid ^{3}He, Physica B, **210**, 338–346 (1995).

[77] Y. Nishida, Is a color superconductor topological? Phys. Rev. D **81**, 074004 (2010).

[78] M. A. Silaev, Spectrum of bound fermion states on vortices in ^{3}He-B, JETP Lett. **90**, 433 (2009).

[79] G.E. Volovik, Localized fermions on quantized vortices in superfluid ^{3}He-B, J. Phys.: Condens. Matter, **3**, 357–368 (1991).

[80] R. Jackiw and P. Rossi, Zero modes of the vortex-fermion system, Nucl. Phys. **B 190**, 681–691 (1981).

[81] G.E. Volovik, Topological invariants for Standard Model: from semi-metal to topological insulator, JETP Lett. **91**, 55–61 (2010); arXiv:0912.0502.